

Materials and Technologies for New Generation Aeroengines

E.N. Kablov, I.M. Demonis, N.V. Petrushin

All-Russian Institute of Aviation Materials (VIAM), Moscow, Russia

E-mail: admin@viam.ru

Abstract

The analysis of modern nickel-base superalloys evolution for casting single-crystal turbine blades was performed. The role of high gradient directional solidification (LMC method) in producing single crystal turbine blades of nickel-based superalloys is discussed. The results were used in computer designing of fifth generation nickel-base single crystal superalloy. <001> single crystals of the designed superalloy were directionally solidified and investigated in as-cast, and heat treated conditions. Creep rupture tests were performed in the temperature interval of 900–1100 °C and included tests longer 1 000 h.

1. Introduction

Development of high effective materials and new technologies for their manufacture and application is the major factor of development of competitive aviation gas turbine engines (GTE). According to CIAM data in the period from 1970 to 2000 dynamics of efficiency increase of aviation engines of different generations was characterized by increase in the maximal gas temperature at the input of the turbine from 1300-1450 K (third generation) up to 1800-1950 K (fifth generation). Such growth has been attained owing to creation of new materials, basically nickel-base superalloys with high operational characteristics, perfection of cooling systems of turbine blades. In promising engines of the sixth generation the gas temperature will increase up to 2000-2200 K due to application in the turbine of single crystal blades from the rhenium and ruthenium alloyed nickel-base superalloys. These alloys have multicomponent composition and two phase microstructure: a γ -solid solution of nickel hardened by fine γ' -precipitates (intermetallic phase on the base of Ni_3Al). If carbon and/or boron are present carbides and borides can additionally form. During high temperature service superalloys gradually decompose, which results in the formation of different topologically close-packed (TCP) phases.

Beginning in the 1960s, the main tendency in the development of nickel base superalloys for casting turbine blades has been an increase in the content of the hardening γ' phase to 60-70% in the matrix γ solid solution. However, researchers tried to increase the temperature of complete dissolution of the γ' phase in the γ solid solution (i.e., the γ' solvus temperature) by increasing the Al concentration; decreasing the Cr content; alloying with refractory transition metals (Mo, W, Nb, Ta, Hf); and by introducing B, Zr, Y, La, or Ce microadditions.

In the technology of production of turbine blades, equiaxial casting is now replaced by directional and single-crystal solidification. The application of blades made of commercial superalloys with a columnar single-crystal structure allowed the input gas temperature to be increased by 100-150°C. To realize the potential possibilities of the single-crystal structure, researchers designed special-purpose first-generation nickel base superalloys; they are intended for casting single crystals and provide an additional ~20°C increase in the blade operating temperature. The absence of high-angle grain boundaries in single crystals excludes the necessity of introduction of C, B, Zr, and Hf to strengthen grain boundaries. In the absence of carbon and boron, researchers could substantially increase the solidus temperature and the resistance to mechanical and thermal fatigue of single crystals due to the elimination of carbides and borides, which are stress concentrators and crack nucleation sites.

Single crystal nickel based superalloys were then improved owing to a radical change in the casting methods, the application of high-purity charge materials, and the use of new alloying additions.

One of the most effective alloying elements was found to be rhenium. Rhenium improves the high temperature strength of superalloys because it raises the solidus temperature, hardens the γ -solid solution of nickel, increases the γ/γ' -lattice misfit and slows down diffusion of the alloying elements [1]. The rhenium concentration reaches 3-4 wt.% in second-generation single-crystal alloys and 5-6 wt.% in third-generation superalloys [1, 2]. These high-rhenium superalloys with a single-crystal structure were designed with a computer [3-5]. To reach optimum alloying, researchers

improved the physicochemical properties (the γ solvus and solidus temperatures) and the structure-phase characteristics (the lattice parameters of the γ and γ' phases, γ/γ' -lattice misfit, and the volume fraction of the γ' phase) via the addition of a higher amount of rhenium (which is the main solid-solution hardening element); a balanced increase in the total amount of refractory (Re, Mo, Ta, W) and γ' -forming (Al, Ta) metals; a decrease in the Cr, Ti, and Hf concentrations; and the elimination of Nb and V from the alloying system. As a result, single crystal rhenium containing alloys with a high level of optimized parameters were produced. However after long holding at high temperature the TCP phases precipitate in the rhenium containing superalloys, which can have a negative effect on the mechanical properties. To stabilize the phase composition and decrease the probability of TCP phase precipitation 2-6 wt.% of Ru are doped [5-8]. Several generations of single-crystal nickel-base superalloys have been developed. Table 1 shows the composition of typical nickel-based single-crystal superalloys for turbine blades.

Table 1: Nominal chemical compositions (wt.%) of some selected nickel based single-crystal superalloys, and their densities

Alloy	Cr	Co	Mo	Re	W	Al	Ti	Ta	Others	Density (g/cm ³)	Generation	Organization
CMSX-2	8	4.6	0.6	-	8	5.6	1	6	-	8.60	1 st	Cannon Muskegon
PWA1480	10	5	-	-	4	5	1.5	12	-	8.70	1 st	Pratt & Whitney
AM3	8	5.5	2.25	-	5	6	2	3.5	-	8.25	1 st	ONERA
MC2	8	5	2	-	8	5	1.5	6	-	8.63	1 st	ONERA
CMSX-4	6.5	9	0.6	3	6	5.6	1	6.5	0.1Hf	8.70	2 nd	Cannon Muskegon
PWA1484	5	10	2	3	5	5.6	-	8.7		8.95	2 nd	Pratt & Whitney
Rene N5	7	8	2	3	5	6.2	-	7	0.2Hf	8.70	2 nd	GE
CMSX-10	2	3	0.4	6	5	5.7	0.2	8	0.03Hf 0.1Nb	9.05	3 rd	Cannon Muskegon
Rene N6	4.2	12.5	1.4	5.4	6	5.75	-	7.2	0.15Hf	8.97	3 rd	GE
TMS-75	3	12	2	5	6	6	-	6	0.1Hf	8.89	3 rd	NIMS
N1	2.5	11	2	9	1.3	5.75	-	8.8	-	9.09	3 rd	VIAM
TMS-138	3.2	5.8	2.8	5	5.9	5.9	-	5.6	2Ru	8.95	4 th	NIMS and IHI
MC-NG	4	0.2	1	4	5	6	0.5	5	4Ru 0.1Hf	8.75	4 th	ONERA
EPM-102/ MX-4/ PWA1497	2	16.5	2	5.95	6	5.55	-	8.25	0.15Hf	9.20	4 th	GE, Pratt & Whitney and NASA
N4	2.5	6.3	4	6	4	6	-	4.5	4Ru	8.87	4 th	VIAM
TMS-162	2.9	5.8	3.9	4.9	5.8	5.8	-	5.6	6Ru 0.09Hf	9.04	5 th	NIMS and IHI
TMS-196	4.6	5.6	2.4	6.4	5	5.6	-	5.6	5Ru 0.1Hf	9.01	5 th	NIMS and IHI

The most high temperature superalloys of last generations contain rhenium and ruthenium. Rhenium-ruthenium-bearing superalloys have improved high-temperature long-term rupture strength, and thermal stability; unlike traditionally alloyed superalloys (CMSX-2, PWA1480), they have higher temperature by ~60 °C (Fig. 1).

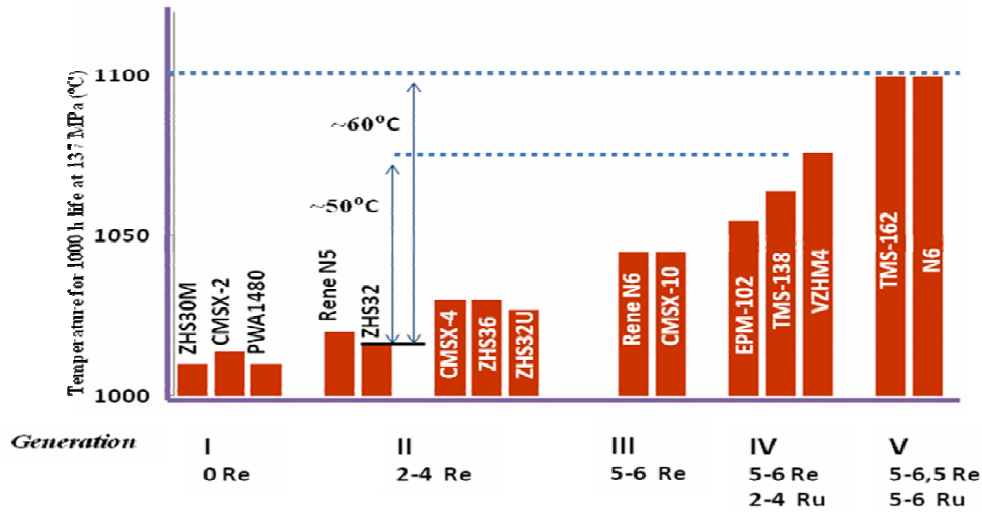


Figure 1: The temperature capability of single crystal nickel-based superalloys.

The experimental results presented in this work were obtained by us at the VIAM, are complemented by the related data of [9-11], and explains the physicochemical principles and technological features used by authors in development of nickel-base superalloys for manufacturing single-crystal blades for aviation gas turbine engines.

2. Alloy design and Development

For a long time, the empirical “trial-and-error” method was the main method used for metal-based high-superalloy development. It is quite apparent that the development of the optimal composition and properties complex for nickel-based superalloys alloyed by more than 15 elements is a highly laborious task requiring much time and financial expenditure. It especially concerns the alloys alloyed with expensive elements such as rhenium, ruthenium, and others. In this connection, the formal methods of computerized design of modern superalloys are the necessary means [15]. Essentially, the traditional “trial-and-error” method is replaced by the proximate and economical method “do rightly from the very first”, which allows us to optimize not only the chemical compositions of already available commercial alloys, but also to develop new ones. General conclusion and analysis of numerous experimental data permit us to determine the influence of alloying elements on the phase composition, physicochemical, structural-phase, thermophysical, and high-temperature properties of nickel-based alloys. As a result of the statistical treatment of numerous experimental data files, the regression equations were derived which permit us to calculate the above-mentioned characteristics for any new nickel-based superalloys being developed. This approach was realized by authors during the development of the computerized design method of cast nickel-based superalloys, which includes the calculation of phase composition, phase stability parameters, physicochemical, structural-phase, thermophysical, and high-temperature characteristics of nickel-based superalloys.

Optimization of the alloy composition was carried out for the nickel-base system Ni–Al–Cr–Mo–W–Ta–Co–Re–Ru by the method of computer design described in [4]. The algorithm of this method consists in following. In the given alloying system the concentration of each alloying element was broken into two levels: minimum and maximum. The complete factorial experiment (CFE) was described by a design matrix of 2^n type, where $n = 8$ is number of the main alloying elements without nickel. The compositions of all 2^n alloys were evaluated by parameter ΔE [12]:

$$\Delta E = E_{\text{alloy}} - E_0 \text{ with } E_0 = 0.036A_{\text{alloy}} + 6.28 \quad (1)$$

where $A_{\text{alloy}} = \sum_{i=1}^n A_i C_i$ is the average atomic mass of alloying element in mole, alloying element in mole,

$E_{\text{alloy}} = \sum_{i=1}^n E_i C_i$ the average number of valence electrons, A_i , E_i and C_i respectively the atomic mass, number of valence electrons and atomic concentration of i -element. Number of valence electrons E_i is presented in Table 2.

Table 2: Number of valence electrons of alloying elements for Ni-based superalloys

Element	Cr	Co	Mo	Re	W	Al	Ti	Ta	Ru	Nb	Hf	Ni
E	6	9	6	7	6	3	4	5	8	5	4	10

The equation for parameter E_0 in (1) is obtained by regression of the experimental data on phase composition for a large group of different nickel-base superalloys. In coordinates $E_0 - A_{\text{alloy}}$ the parameter E_0 determines the boundary of phase stability of the γ/γ' -microstructure of a nickel-base superalloy. For commercial nickel-base superalloys the value of E_{alloy} usually differs slightly from E_0 by $\pm\Delta E$, called the ‘‘alloying imbalance’’. The sign and value of ΔE determines the probability of formation of different undesirable phases. For example, in alloys with a large negative alloying imbalance ($\Delta E < 0$) the probability of formation of carbides such as M_6C or TCP phases is high. Alloys with $\Delta E > 0$ are disposed to form such phases as Ni_3Ti and Ni_3Nb or eutectic (peritectic) phases on the base of Ni_3Al . If $\Delta E = 0$ the alloy is accepted as a balanced one. In this work the alloy composition was accepted as balanced (i.e. the alloy has only γ - and γ' -phases) if the condition $-0.04 \leq \Delta E \leq 0$ was fulfilled. The physicochemical and structural parameters of single-crystal nickel-base superalloys (γ' -solvus temperature, melting temperature of nonequilibrium eutectic $\gamma+\gamma'$, solidus temperature, liquidus temperature, γ/γ' -lattice misfit, γ' -volume fraction, diffusion factors etc) of the alloy were calculated by regression equations obtained in [4].

Figure 2 shows experimental data on the partitioning coefficient of alloying elements between the γ' - and γ - phases for a large group of different nickel-base superalloys [9, 11].

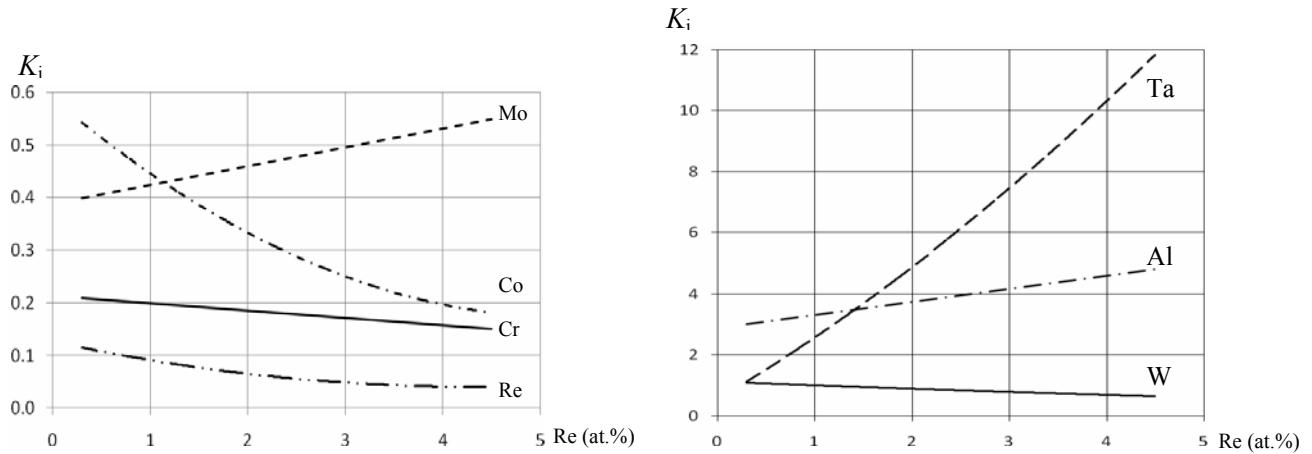


Figure 2: The effect of rhenium on the partitioning coefficient of alloying elements between the γ' - and γ -phases in nickel-base superalloys.

The partitioning coefficient K_i is defined as $K_i = C_{i\gamma'} / C_{i\gamma}$, where $C_{i\gamma'}$ and $C_{i\gamma}$ are the atomic concentration of the alloying element i in the γ' - and γ -phases, respectively. It is seen that rhenium significantly influences the partitioning coefficient of tantalum, titanium, aluminum, cobalt and itself rhenium. With an increase in the rhenium concentration K_{Ta} , K_{Ti} and K_{Al} increase while K_{Co} and K_{Re} decrease. The dependence of $K_{Re} = f(C_{Re})$ looks like a monotonically decreasing function asymptotically approaching 0.05. The partitioning coefficients of other alloying elements (Cr, Mo, Nb, and V) show a weak dependence on the rhenium concentration. It should be mentioned that in nickel-base superalloys with high rhenium concentration $K_W < 1$. The dependence $K_{Ta} = f(C_{Re})$ is of special interest. An increase in rhenium concentration in the alloy leads to a displacement of tantalum from the γ -solid solution into the γ' -phase. The increases in tantalum concentration in the γ' -phase and rhenium in the γ -phase have positive influences on both phases, which improves the mechanical properties of alloy. It should be mentioned however that a displacement of tantalum from the γ -phase into the γ' -phase decreases the γ -lattice spacing and increases the γ' -lattice spacing. This results in a decrease in the absolute value of γ/γ' -misfit, which can reach zero or even become positive ($a_\gamma < a_{\gamma'}$). In this case the γ' -precipitates take the adverse spherical shape.

The value of the γ/γ' -misfit was the main factor determining the choice of the best alloy composition among the stable phase compositions defined by parameter ΔE ($-0.04 \leq \Delta E \leq 0$). It was assumed that the γ/γ' -misfit improves the

creep strength and in the given alloying system its value should be at least 2–3 times higher than that in the single-crystal nickel-base superalloys of the second and third generations.

Additional factors considered in the alloy evaluation were: γ' -solvus temperature T_{solvus} , γ' -volume fraction F_0 , alloy density ρ , melting temperature of nonequilibrium eutectic $\gamma+\gamma'$ T_{eutectic} , solidus temperature T_S , liquidus temperature T_L , heat treatment window $T_{\text{eutectic}}-T_{\text{solvus}}$, castability (“freckles” formation), parameters etc., 15 factors in total. The chemical composition of the chosen alloy N6 is presented in Table 3. Table 4 gives some physicochemical characteristics predicted for this alloy in comparison with the experimental data.

Table 3. Chemical composition for designed alloy N6[®] and alloys N4[®] [11] in wt.%

Alloy	Cr	Co	Mo	Re	W	Al	Ta	Ru	Ni
N6	3	5.5	3.3	6.3	4	5.7	5.8	5	Base
N4	2.5	6.3	4	6	4	6	4.5	4	Base

Table 4: Properties of designed alloy N6

	Designed	Experimental
Physicochemical characteristics:		
ρ (g·cm ⁻³)	9.11	9.03
T_{solvus} (°C)	1 324	1 328
T_{eutectic} (°C)	1 337	1 340
T_S (°C)	1 379	1 376
T_L (°C)	1 437	1 422
Structural characteristics:		
F_0 (vol.% at 850 °C)	61.1	64.2
F_{eutectic} (vol.%)	3.3	1.7
δ (% at R.T.)	-0.49	-0.45
Phase stability parameters:		
ΔE	-0.06	-
Creep strength: σ_{1000}^{1000} (MPa)	225	220
<i>Note:</i> ρ is density; T_{solvus} – temperature of γ' -solvus; T_{eutectic} – melting temperature of nonequilibrium eutectic $\gamma+\gamma'$; T_S – solidus temperature; T_L – liquidus temperature; F_0 – γ' -volume fraction; F_{eutectic} – volume fraction of nonequilibrium eutectic $\gamma+\gamma'$; δ – γ/γ' -lattice misfit is defined $\delta = (a_{\gamma'} - a_{\gamma})/0.5(a_{\gamma'} + a_{\gamma})$, a_{γ} is the γ -spacing, $a_{\gamma'}$ the γ' -spacing; σ_{1000}^{1000} – 1 000-h rupture stress at 1 000 °C for <001> single crystals.		

2.1. Solidification of single-crystals

Successful development of high-superalloys should be impossible without creation of a special technology of single-crystal casting. At present, VIAM is the only enterprise in the world that has developed and uses the high-gradient technology and special equipment for manufacturing the single-crystal turbine blades by directional solidification method [13]. In the manufacture of single-crystal blades from superalloys according to the available in the industry directional solidification methods with low-temperature gradient (10-30 °C·cm⁻¹), the size of the solid–liquid zone in the casting being solidified achieves tens of millimeters. Consequently, because of overlapping interdendritic channels by the second-order dendritic cores, the melt flow in them becomes difficult. As a result, during the solidification of interdendritic liquid, the interdendritic pores are formed in consequence of the molar volume differences of liquid and solid phases. In addition, the casting produced by low-gradient technology is characterized by a coarse dendritic structure (distance between primary dendrite axes achieves 400–800 μm) with developed second-order axes. At this point, the higher segregation of alloying elements takes place, which results in the formation of large precipitates of the eutectic origin phases in the interdendritic regions. It should be noted that in the manufacturing blades of rhenium-bearing superalloys, by this technology it is impossible to eliminate completely the formation of growth defects such as “freckles”, which disrupt the single-crystal structure of blades. In the case of the high-gradient method of directional

solidification (LMC method: liquid metal cooling) with temperature gradient of $\sim 200\text{ }^{\circ}\text{C}\cdot\text{cm}^{-1}$, the size of the solid–liquid zone decreases. As a result, the dendritic segregation substantially decreases that leads to the reduction of micropore size and volume fraction. In this case, in the single-crystal casting, the following phenomena are observed: the formation of a more homogeneous structure of the superalloy with significantly small distances (2–3 times) between dendrite axes, the formation of eutectic origin nonequilibrium phases is suppressed, and the formation of “freckles”-type defects is totally eliminated. The process of high-gradient directional solidification permits us to produce the blades of nickel-based superalloys with a high content of rhenium having essentially more perfect single-crystal structure and makes their heat treatment more economic.

In present work single-crystal bars of the designed superalloy N6 (\varnothing 16 mm and length 185 mm) were directionally solidified in $\langle 001 \rangle$ direction by the LMC method. The $\langle 001 \rangle$ growth was initiated by a seed of a high temperature Ni–W alloy placed in a special cavity of the ceramic mould. The single-crystals grown under given solidification conditions have a typical dendritic-cellular macrostructure with a primary dendrite arm spacing of about $250\text{ }\mu\text{m}$ (see Fig. 3a).

2.2 Microstructure and dendritic segregation

The solidified castings contain $\sim 2\text{ vol.}\%$ of nonequilibrium eutectic $\gamma'+\gamma$ (or peritectic phase γ') in the interdendritic regions (Fig. 3b).

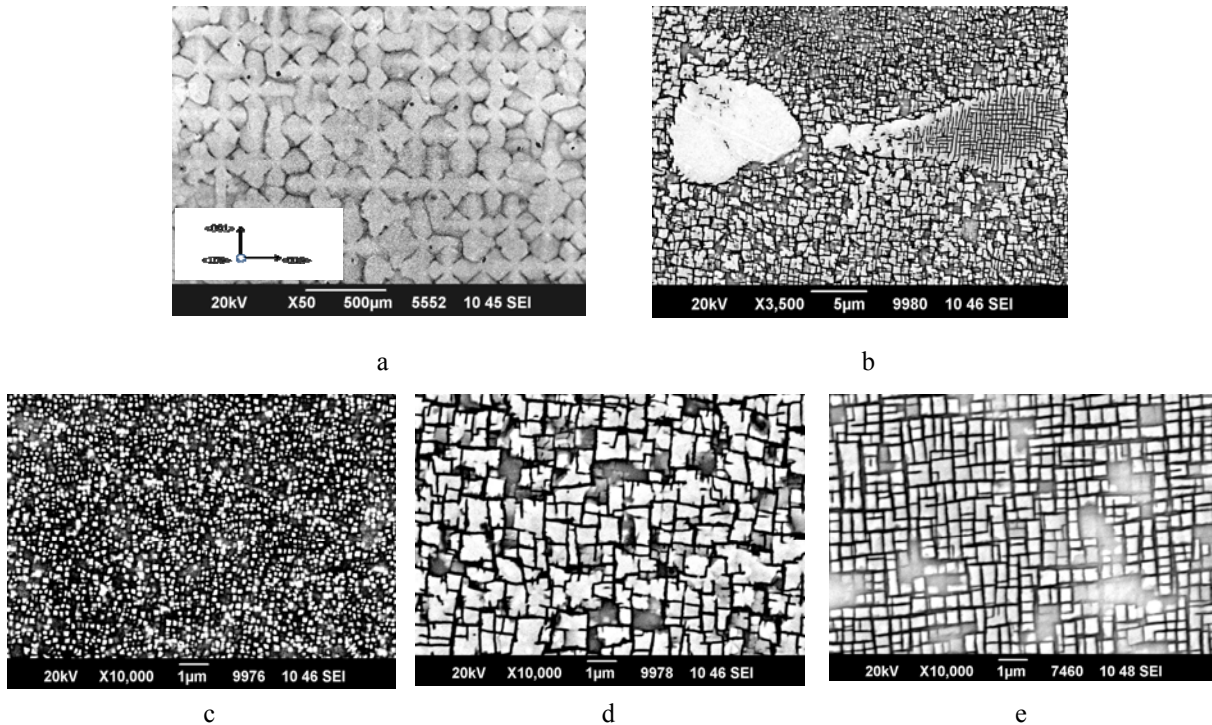


Figure 3: Microstructure of single crystal of N6 alloy after cast (a-d) and heat treatment (e):
 (a) dendrite macrostructure; (b) eutectic (peritectic) $\gamma+\gamma'$ precipitates in the interdendritic region;
 γ' - precipitates in the (c) dendrite axis (PDA) and interdendritic region (d); (e) γ/γ' -microstructure.

The size and shape of γ' - precipitates essentially differ in the dendrite axes and interdendritic regions (Fig. 3 c and d). In the last ones the γ' -precipitates are 3–5 times larger than in the dendrite axes and have less pronounced the cuboidal morphology. This dimensional and morphological inhomogeneity results from the segregation of alloying elements during dendritic growth. The dendritic segregation was characterized by coefficients K_s :

$$K_s = C_{\text{IR}}/C_{\text{PDA}} \quad (2)$$

where C_{IR} and C_{PDA} are respectively the local concentrations of alloying elements in the interdendrite regions (IR) and the primary dendrite axes (PDA). In such a definition the value of a segregation coefficient is >1 when the alloying

element enriches the interdendritic regions (so-called direct segregation). In the case of inverse segregation the alloying element concentrates in the dendrite axes and the coefficient is <1. The values of segregation coefficients measured in superalloy N6 are presented in Table 5.

Table 5: Coefficients of dendritic segregation of alloying elements of single crystals nickel-base superalloy N6

$K_s = C_{IR}/C_{PDA}$							
Cr	Mo	Al	W	Ta	Co	Re	Ru
1.0	1.2	1.3	0.5	2.1	0.8	0.3	0.9

One can see in Table 5 that rhenium and tungsten strongly segregate in the dendrite axes while tantalum and aluminium strongly segregate in the interdendritic regions. Chromium, cobalt, molybdenum and ruthenium segregate weakly, slightly enriching the dendrite axes. Figure 3 (e) shows the microstructure of superalloy N6 after full heat treatment: a 26 h long multistep homogenization in the temperature interval of 1 285–1 320 °C followed by a two step ageing. During homogenization first the nonequilibrium eutectic $\gamma+\gamma'$ dissolves and then the chemical composition within a dendritic cell homogenizes. Solution of the $\gamma+\gamma'$ eutectic results in the formation of micropores in the interdendritic regions. After full heat treatment the differences in γ' -shape and size in the dendrite axes and interdendritic regions become smaller. Over the whole dendritic cell the γ' -precipitates have cuboidal morphology and size of 0.4–0.5 μm (Fig. 3 e). The segregation coefficients of rhenium and tungsten decrease, respectively, to values of 0.7 and 0.9. The concentrations of other alloying elements are nearly completely equalized. Thus the remaining microstructural inhomogeneity (slight difference in the γ' -shape and size) is obviously an effect of the remanent rhenium segregation, which has extremely low diffusion mobility in nickel.

2.3 Creep strength

<001> single-crystals of the superalloy N6 were tested under creep conditions at temperatures 900, 1 000 and 1 100 °C (within the range of tolerance $\pm 10^\circ$) until rupture. The results of performed tests were fitted by equation [14]:

$$\tau = \zeta T^m \sigma^{-n} \exp\left(\frac{U_0 - \eta\sigma}{RT}\right) \quad (3)$$

where τ is creep lifetime in hour; σ stress in MPa; T temperature in K; ζ , m , n , U_0 (activation energy in $\text{J}\cdot\text{mol}^{-1}$), η (activation volume in $\text{J}\cdot(\text{mol}\cdot\text{MPa})^{-1}$) adjustable parameters; R – universal gas constant in $\text{J}\cdot(\text{K}\cdot\text{mol})^{-1}$.

Using the obtained values of adjustable parameters the levels of rupture stress (σ_r) were calculated for lifetimes $\tau = 100$ and 1 000 hours at 900, 1 000 and 1 100 °C. The determined levels of rupture stress for superalloy N6 are presented in Table 6 in comparison with those for some superalloys of the fourth and fifth generations. The chemical composition of the single crystal Ni-base superalloy N4 is presented in Table 2, alloys EPM-102 and TMS-162 – in Table 1.

Table 6: Creep strength of superalloy N6 in comparison with other single crystal nickel-base superalloys

Alloy	Generation	T (°C)	σ_{100} (MPa)	σ_{1000} (MPa)	Ref.
N6	5 th	900	595	435	This work
		1 000	315	220	
		1 100	180	130	
N4	4 th	900	575	410	[11]
		1 000	305	200	
		1 100	170	120	
EPM-102	4 th	900	503	385	
		1 000	325	200	
		1 100	148	97	
TMS-162	5 th	900	565	425	[15]
		1 000	320	230	
		1 100	180	135	

Thus, the results allow us to conclude that the designed rhenium and ruthenium containing superalloy N6 possesses high structural and phase stability. At 1 100 °C this superalloy has higher creep strength than the known superalloys of the third and fourth generations and it is highly competitive with the known fifth generation superalloys containing rhenium and ruthenium.

3. Conclusions

1. The new single crystal nickel-base superalloy N6 containing 6.3 wt.% Re and 5 wt.% Ru is designed on the basis of calculations of the phase composition, physicochemical and structural parameters of the nickel-based system Ni–Al–Cr–Mo–W–Ta–Co–Re–Ru. High phase stability and creep strength of this superalloy are achieved by the balance of the total concentrations of refractory (Re, Ru, Mo, Ta, W) and γ' -forming (Al, Ta) elements.

2. The rhenium and ruthenium superalloy N6 is phase stable during creep tests at 1 100 °C longer than 1 000 h. The main factors decreasing the creep strength at this temperature are: solution of strengthening γ' -phase and corresponding increase in γ -volume fraction, degradation of γ/γ' -microstructure and microporosity.

4. References

- [1] Kablov, E.N., N.V. Petrushin, L.B. Vasilenok, and G.I. Morozova. 2000. Rhenium in Nickel Superalloys for Gas-Turbine Blades. *Materialovedenie*. No 2: 23-29; No 3: 38-43.
- [2] Erickson, G.L., A New Third Generation Single Crystal Casting Superalloy. 1995. *J. of Metals*. V. 47, No 4: 36-39.
- [3] Hino T., T. Kobayashi, Y. Koizumi, H. Harada, and T. Yamagata. 2000. Development of a New Single Crystal Superalloy for Industrial Gas Turbines. In: T.M. Pollock, R.D. Kissinger, R.R. Bowman, K.A. Green, M. McLean, S.L. Olson, J.J. Schirra. (Eds.). *Superalloys 2000*. TMS, Warrendale, PA. 729-736.
- [4] Kablov, E.N. and N.V. Petrushin. 2006. Computer Method of Designing Casting Nickel Superalloys. In: *Casting Superalloys: Kishkin's Effect*. Nauka, Moscow. 56-78.
- [5] Caron, P. 2000. High γ' Solvus New Generation Nickel-based Superalloys for Single Crystal Turbine Blade Applications. In: T.M. Pollock, R.D. Kissinger, R.R. Bowman, K.A. Green, M. McLean, S.L. Olson, J.J. Schirra. (Eds.). *Superalloys 2000*. TMS, Warrendale, PA. 737-746.
- [6] Walston S., A. Cetel, R. MacKay, K. O'Hara, D. Duhl, R. Dreshfield. 2004. Joint Development of a Fourth Generation Single Crystal Superalloy. In: K.A. Green, T.M. Pollock, H. Harada, T.E. Howson, R.C. Reed, J.J. Schirra, S. Walston (Eds.). *Superalloys 2004*. TMS, Warrendale, PA. 15-24.
- [7] Koizumi Y., T. Kobayashi, T. Yokokawa, J. Zhang, M. Osawa, H. Harada, Y. Aoki, M. Arai. 2004. Development of Next-generation Ni-base Single Crystal Superalloys. In: K.A. Green, T.M. Pollock, H. Harada, T.E. Howson, R.C. Reed, J.J. Schirra, S. Walston (Eds.). *Superalloys 2004*. TMS, Warrendale, PA. 35-43.
- [8] Sato A., H. Harada, An-C. Yeh, K. Kawagishi, T. Kobayashi, Y. Koizumi, T. Yokokawa, and J.-X. Zhang. 2008. A 5th Generation SC Superalloy with Balanced High Temperature Properties and Processability. In: R.C. Reed, K.A. Green, P. Caron, T.P. Gabb, M.G. Fahrman, E.S. Huron, S.A. Woodard (Eds.). *Superalloys 2008*. TMS, Warrendale, PA. 131-138.
- [9] Kablov E.N., N.V. Petrushin. 2004. Physicochemical and Technological Features of Creating Metal-Based High-Superalloys. *Pure Appl. Chem.* 76, No.9: 1679-1689.
- [10] Petrushin N.V., I.L. Svetlov, A.I. Samoylov, O.B. Timofeeva, E.B. Chabina. 2008. High-Temperature Phase and Structure Transformations in Single Crystals of Nickel Superalloy Containing Rhenium and Ruthenium. 2008. *Materialovedenie*, No.10: 13-18; No.11: 26-31.
- [11] Petrushin N.V., I.L. Svetlov, A.I. Samoylov, G.I. Morozova. 2010. Physicochemical Properties and Creep Strength of a Single Crystal of Nickel-base Superalloy Containing Rhenium and Ruthenium. *Int. J. Mat. Res. (formerly Metallkd.)*. 101, No.5: 594-600.
- [12] Morozova G.I. 1991. Formation of the Chemical Composition of the γ/γ' Matrix of Multicomponent Nickel Alloys. *Dokl. Akad. Nauk SSSR*. 320: 1413-1416.
- [13] Kablov E.N. 2001. *Gas Turbine Cast Blades (Alloys, Technology, Coatings)*, p.632, Institute of Steels and Alloys, Moscow.
- [14] Kablov E.N., E.R. Golubovsky. 1998. *High-Temperature Strength of Nickel Alloys*, p.464, Mashinostroenie, Moscow.
- [15] Kablov E.N., N.V. Petrushin, and I.L. Svetlov. 2006. Computer Design of a Fourth-Generation Nickel Superalloy for Single-Crystal Gas-Turbine Blades. In: *Casting Superalloys: Kishkin's Effect*. Nauka, Moscow. 98-115.